

## APPLICATIONS OF PURE AND COMBINED BUCKLING MODE CALCULATION OF THIN-WALLED MEMBERS USING THE FINITE ELEMENT METHOD

**Gustavo P. Mezzomo\*, Ignacio Iturrioz\* and Gladimir de C. Grigoletti\*\***

\* Postgraduate Program in Mechanical Engineering (PROMEC), Federal University of Rio Grande do Sul (UFRGS) - Brazil

e-mails: gpmezzomo@yahoo.com.br, ignacio@mecanica.br

\*\* Civil Engineering Course, Lutheran University of Brazil (ULBRA) - Brazil

e-mail: grigoletti@cpovo.net

**Keywords:** Thin-Walled Members, Pure Buckling Modes, Constraints.

***Abstract.** Cold-formed steel members are characterized by the slenderness and the facility of fabrication in different geometries. On the other hand, the use of slender members results in the interaction of different buckling modes, making the analysis of thin-walled members a complex task. Pure buckling mode calculation helps in better understanding the behavior of these members. In this paper, the critical buckling load calculation of specific and combined modes has been carried out using the finite element method for a lipped channel section subjected to a compressive axial load. The deformation fields of the finite element model are constrained according to the analyzed mode. The combined mode calculation enables the quantification of the interaction between the considered modes. Results for two different boundary condition configurations of member ends are shown. Finally, the potentiality of the procedure proposed herein is discussed.*

### 1 INTRODUCTION

Cold-formed steel members, or thin-walled members, are characterized by the slenderness and by the facility of production in different cross-sectional geometries. These members are a thin and economic option for the modern steel construction. On the other hand, the use of thin plates in the fabrication of these members results, many times, in a high width-to-thickness ratio of the plate elements that make up the section. Therefore, besides global buckling, cold-formed members under compressive stresses are very susceptible to the local buckling of plate elements and to distortional buckling of the cross-section.

Although global, distortional and local modes are widely accepted phenomena that are normally handled in design specifications, there are no general methods for the calculation of these three characteristic modes. Furthermore, there is a lack of clear definitions for these three types of *pure buckling modes*. Bearing in mind that these pure modes can interact, we can say that the analysis of thin-walled members is at least complex.

Numerical methods are usually used in the analysis of thin-walled members, namely the finite element method (FEM), the finite strip method (FSM) [1] and the generalized beam theory (GBT) [2]. The GBT is the only known method that inherently can produce and isolate solutions for all common buckling modes: global, distortional or local. However, its applications are limited. The ideal scenery in the analysis of cold-formed members would be a general solution method, like FEM, that could give us the critical loads of pure buckling modes.

Ádány and Schafer [3] have proposed a new approach that enables the decomposition of a stability problem solution of an open cross-section thin-walled member into pure buckling modes, or into

*individual modes* (modes inside the vector space of a pure mode). The definitions of pure buckling modes rely on mechanical assumptions of GBT. The deformation field of the numerical model is then constrained in accordance with the assumptions that underlie global (G), distortional (D), local (L) or other (O) modes. The implementation of these concepts has been accomplished in the FSM context, by the use of CUFSM software [1], giving rise to the constrained finite strip method (cFSM). More recently, a proposal of extending the constraining process of cFSM to FEM has been presented by Casafont *et al.* [4]-[5]. The procedure allows the critical load calculation of individual buckling modes through the constraining of finite element models.

This paper aims to obtain the critical loads of individual or combined buckling modes of open cross-section thin-walled members, by constraining finite element models. With this goal, general concepts of the constraining procedure of Ádány and Schafer have been used, and a methodology using Ansys software (<http://www.ansys.com/>), similar to that of Casafont, has been employed. The combined mode calculation using the presented procedure enables the quantification of the interaction between modes.

Taking a lipped channel section in pure compression as example, the critical load calculation of individual G, D and L modes and a combination of D and L modes has been accomplished. Two different boundary condition configurations of member ends have been considered.

## 2 CONSTRAINED STABILITY PROBLEM

This section introduces the basic constraining procedure of a stability problem that provides means for the solution to be focused on a pure buckling mode (or on a combination of any individual modes). The procedure is the same that has been proposed by Ádány and Schafer [3] for the cFSM. Mechanical assumptions of GBT are used to define the pure G and D modes. If some of these assumptions are released, it is also possible to define L and O modes.

The mechanical assumptions that underlie the pure modes are employed as constraint equations on the deformation fields. Therefore, the general degrees of freedom (DOFs) of the problem, denoted by vector  $\mathbf{d}$ , can be related to a reduced number of DOFs that define the deformation field constrained according to a pure mode (vector  $\mathbf{d}_M$ ). For this, a constraint matrix  $\mathbf{R}_M$  is defined as in Eq. (1). The subscript M represents the constraint to a pure buckling mode: G, D, L or O. Thus, one can construct constraint matrices associated to each of these buckling modes.

$$\mathbf{d} = \mathbf{R}_M \mathbf{d}_M \quad (1)$$

The linear stability problem (generalized eigenvalue problem) given by Eq. (2) can be focused on a pure buckling mode through the application of Eq. (1), resulting in a constrained eigenvalue problem, which is given by Eq. (3).  $\mathbf{K}_e$  is the elastic stiffness matrix,  $\mathbf{K}_g$  is the geometric stiffness matrix,  $\mathbf{K}_{e,M} = \mathbf{R}_M^T \mathbf{K}_e \mathbf{R}_M$ ,  $\mathbf{K}_{g,M} = \mathbf{R}_M^T \mathbf{K}_g \mathbf{R}_M$  and  $\lambda$  is an eigenvalue that satisfies the considered equation.

$$\mathbf{K}_e \mathbf{d} = \lambda \mathbf{K}_g \mathbf{d} \quad (2)$$

$$\mathbf{K}_{e,M} \mathbf{d}_M = \lambda \mathbf{K}_{g,M} \mathbf{d}_M \quad (3)$$

After solving Eq. (3), the pure mode can be described by general DOFs of the model through Eq. (1). Thus,  $\mathbf{d}_M$  can be interpreted as a vector of generalized coordinates, depending on the basis used for defining the  $\mathbf{R}_M$  matrix. The columns of  $\mathbf{R}_M$  are individual deformation modes that form a basis for the reduced space of the pure mode M. The G, D, L and O spaces together span the entire space of original DOFs of the problem, or, in other words, they represent a transformation of the solution to a basis where G, D, L and O spaces are segregated (Eq. (4)).

Eq. (4) clearly shows that one can define a generic constraint matrix using any of the columns of  $\mathbf{R}_G$ ,  $\mathbf{R}_D$ ,  $\mathbf{R}_L$  and  $\mathbf{R}_O$ . It means that it is possible to construct a constrained eigenvalue problem as in Eq. (3) whereby the solution is focused on any individual deformation mode or on any combination of individual

modes. Additional transformations inside G, D, L and O spaces are possible. If orthogonal deformation modes are used in the definition of the constraint matrices of Eq. (4), and a normalization scheme is applied (orthonormal bases), the vector  $\{d_G \ d_D \ d_L \ d_O\}^T$  will give the contribution of each individual deformation mode for the general solution of the problem of Eq. (2) (buckling mode).

$$d = \left[ \begin{matrix} R_G & R_D & R_L & R_O \end{matrix} \right] \begin{Bmatrix} d_G \\ d_D \\ d_L \\ d_O \end{Bmatrix} \quad (4)$$

Orthogonal bases for G, D, L and O spaces can be defined from the eigenvectors of Eq. (3). The procedure is described in [3], where these modal bases are called *orthogonal axial modes*, since they are defined for a member under axial load. Three normalization schemes are used in CUFSM:

1. *Vector norm* (VN): the base vectors are normalized by setting  $d^T d = 1$ .
2. *Strain energy norm* (SEN): the base vectors are normalized by setting  $d^T K_e d = 1$ .
3. *Work norm* (WN): the base vectors are normalized by setting  $d^T K_g d = 1$ .

### 3 METHODOLOGY

#### 3.1 Model under study

In this paper, the analyses have been carried out for a lipped channel section subjected to uniformly distributed compressive axial loads at the member ends. Fig. 1(a) shows the section dimensions in mm. The section is the same that has been studied by Casafont *et al.* in [4].

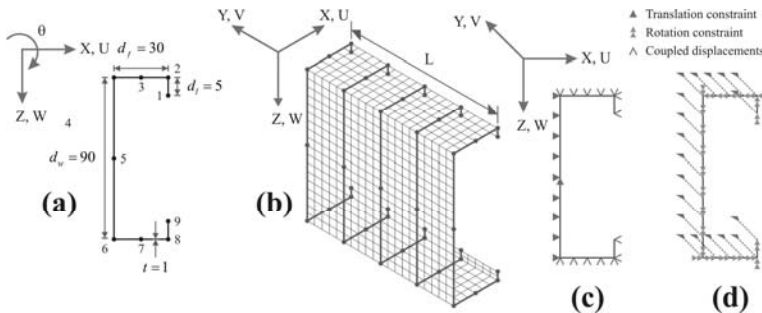


Figure 1: (a) Analyzed cross-section. (b) Finite element mesh. (c) End boundary conditions for a simply supported member. (d) Additional end boundary conditions for a clamped member.

The member has been modeled using 4-node, 24-DOFs shell elements, with a maximum size of 5 mm, with the use of Ansys. Fig. 1(b) illustrates the finite element mesh of a member with an arbitrary length L. Figs. 1(a) and 1(b) indicate the DOFs utilized in the derivation of the constraint matrices (U, V, W e  $\theta$ ); these are the FSM DOFs. It should be noted that the coordinate system is the same of [3].

Two different kinds of boundary conditions have been considered: (1) simply-simply supported member (S-S) and (2) clamped-clamped supported member (C-C). The boundary conditions at the model ends for the S-S member are shown in Fig. 1(c), where the Poisson effect is free to take place. Besides the boundary conditions already shown in Fig. 1(c), the constraints of Fig. 1(d), regarding local rotation of the plates and the warping, must be added at the ends of C-C member model.

A linear buckling analysis has been carried out in order to obtain the critical loads. First, a linear elastic analysis is performed, giving rise to the geometric stiffness matrix. Subsequently, an eigenvalue problem is solved to obtain the buckling modes and the associated critical loads. It should be pointed out

that, for the C-C member, the null warping at member ends can only be applied after the linear elastic analysis. For the S-S member, any longitudinal constraint should be deleted after the linear elastic analysis, unless the warping of the analyzed mode is null where the constraints are applied.

### 3.2 Constraining the finite element mesh

This section presents the methodology employed to constrain the finite element models according to individual or combined buckling mode. The constraint matrices of Eqs. (1) and (4) have been derived at cross-section level in [3], where the context has been the FSM. In order to extend the constraining procedure to the FEM, the variation of displacements along the member length must be considered.

As an example, Eq. (4) is written using only two columns of constraint matrices (individual orthonormal modes) and taking into account the longitudinal variation of displacements (Y direction). At this point, it is important to treat transversal DOFs (U, W and  $\theta$ ) and longitudinal DOFs (V) separately:

$$d(Y) = \begin{Bmatrix} U(Y) \\ V(Y) \\ W(Y) \\ \theta(Y) \end{Bmatrix} = [R_1(Y) \ R_2(Y)] \begin{Bmatrix} \beta_1 \\ \beta_2 \end{Bmatrix} = \begin{bmatrix} R_{U1}\psi_1(Y) & R_{U2}\psi_2(Y) \\ R_{V1}\psi_1'(Y)(L/r_1\pi) & R_{V2}\psi_2'(Y)(L/r_2\pi) \\ R_{W1}\psi_1(Y) & R_{W2}\psi_2(Y) \\ R_{\theta 1}\psi_1(Y) & R_{\theta 2}\psi_2(Y) \end{bmatrix} \begin{Bmatrix} \beta_1 \\ \beta_2 \end{Bmatrix} \quad (5)$$

$\beta_1$  and  $\beta_2$  are the contribution coefficients of modes  $R_1(Y)$  and  $R_2(Y)$ ;  $\psi_1(Y)$  and  $\psi_2(Y)$  are the functions defining the variation of displacements in Y direction of Fig. 1 (*shape functions*), which are usually assumed to be harmonic;  $r_1$  and  $r_2$  are the numbers of half-waves of the two considered functions. The columns of the constraint matrices have been partitioned into vectors referring to the different types of DOFs. It should be noted that V DOFs vary according to the derivatives of  $\psi_1(Y)$  e  $\psi_2(Y)$ . Shape functions for different kinds of boundary conditions of member ends can be found in [6].

Since it is not possible to transform the stiffness matrices in Ansys (as in Eq. (3)), the constraints have to be applied through DOFs relationships between the nodes. Eq. (5) gives the distribution of displacements U, V, W and  $\theta$  at a generic section of the model. Recognizing this, one DOF of each section must be assumed as the unknown DOF in the eigenvalue analysis. As U, W and  $\theta$  have a longitudinal variation that is different from that of V, it is appropriate to uncouple V from the other DOFs. Therefore, two unknown DOFs per section are considered.

The DOFs V and  $\theta$  of node 1 of each section (Fig. 1(a)) are chosen to be the unknowns. Thus, the DOF  $V_{is}$ , corresponding to a node i of a section s, can be expressed in function of  $V_{1s}$  (node 1 of section s) as shown in Eq. (6).  $R_{V1,i}$ ,  $R_{V2,i}$ ,  $R_{V1,1}$  and  $R_{V2,1}$  are components of vectors  $R_{V1}$  e  $R_{V2}$  referring to nodes i and 1;  $Y_s$  is the coordinate of the section in the model.

$$V_{is} = \frac{\beta_1 R_{V1,i} \psi_1'(Y_s)(L/r_1\pi) + \beta_2 R_{V2,i} \psi_2'(Y_s)(L/r_2\pi)}{\beta_1 R_{V1,1} \psi_1'(Y_s)(L/r_1\pi) + \beta_2 R_{V2,1} \psi_2'(Y_s)(L/r_2\pi)} V_{1s} \quad (6)$$

The generic DOFs  $U_{is}$ ,  $W_{is}$  and  $\theta_{is}$  must be related to  $\theta_{1s}$  similarly as in Eq. (6). Reading this equation, it can be noted that if just one unknown per section is chosen (e.g.,  $\theta_{1s}$ ), a ratio between shape functions and its derivatives will be set, thereby prohibiting application of constraints at some coordinates  $Y_s$  [4].

It is also interesting to observe that if only one deformation mode is considered in the analysis (constraint matrix with only one column), the approach that uses two unknowns per section results in a solution with a number of half-waves directly calculated by the FEM program.

Two constraining schemes have been used herein. The first is the same that has been used by Casafont *et al.* in [4]-[5], whereby only a few nodes of a few sections of the model are constrained. Fig. 1(a) exhibits the 9 constrained nodes of each section, with only one intermediary node (subnode) in the web and the flanges. The constraints have been applied every 10 mm for members with  $L \leq 200$  mm and every 25 mm when  $L > 200$  mm (see an example of marked sections in Fig. 1(b)). In the second scheme,

all nodes of the mesh have been constrained. It should be remarked that although all the nodes have been constrained, the constraints have been applied only to the FSM DOFs, i.e., two DOFs per node have remained free. Throughout this paper, the first scheme is called “1 Sub” and the second “Fully”.

The individual deformation modes (columns of the constraint matrix) used in the analyses herein have been taken from the routines of CUFSM software, implemented in Matlab (<http://www.mathworks.com/>) and freely available from Schafer in <http://www.ce.jhu.edu/bschafer/cufsm/>. For G and D modes, only the warping distributions have been taken (DOFs V), since the other DOFs (U, W and  $\theta$ ) can be expressed as a function of V [3]. Therefore, for these modes, U, W and  $\theta$  have been internally determined in Ansys by accessing the stiffness matrices in a substructure analysis.

In order to calculate the contributions of the individual deformation modes in a buckling mode (coefficients  $\beta$  in Eq. (5)), an optimization using the genetic algorithms method has been conducted. The coefficients have been combined such that the critical load has been minimized. The implementation has been carried out in Matlab.

### 4 RESULTS

Fig. 2 illustrates the critical load results of individual deformation modes for the S-S member, using the constraining schemes 1 Sub and Fully. A comparison with results provided by cFSM (CUFSM) and GBT using GBTUL software (<http://www.civil.ist.utl.pt/gbt/>) has been made. In order to compare the results to the ones provided by CUFSM, buckling taking place in only one half-wave along the member length has been considered. Thus, results have been presented as a function of the buckling length.

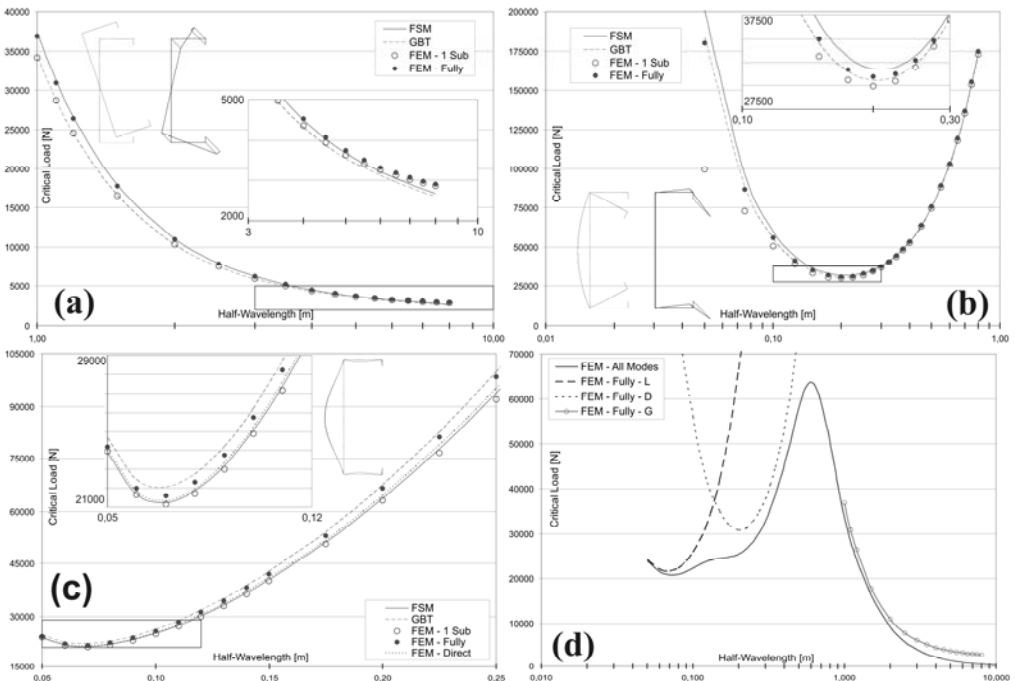


Figure 2: Critical loads of individual deformation modes for the S-S member. (a) First G mode. (b) First D mode. (c) First L mode. (d) Individual modes results comparison with all modes curve.

Using the *orthogonal axial modes* [3] taken from the CUFSM routines, results have been obtained for the first G mode (flexural-torsional), the first D mode and the first L mode (Figs. 2(a), 2(b) and 2(c),

respectively). The transversal deformations of each individual mode along with the warping distributions (zero for the L mode) are exhibited in the insets of the corresponding charts, with an arbitrary magnitude. It should be noted that the distributions of transversal displacements for L mode depends on the half-wavelength. Nevertheless, this dependency is weak for lengths of practical importance. In Fig. 2(c), the L mode for a buckling length of 100 mm is shown.

In Fig. 2(d), the critical load results of individual G, D and L modes obtained using the Fully scheme are compared with the finite element results considering the contribution of all modes, i.e., results of an unconstrained analysis. In this chart, it is possible to have an idea of the interaction between the modes.

In Fig. 2(c), an alternative constraining scheme, compatible with L deformation modes, has been employed (“Direct” scheme). Constraints have been applied directly to the DOFs of the model, as depicted in Fig. 3. Firstly, a linear elastic analysis is solved, giving rise to the geometric stiffness matrix (Fig. 3(a)). Subsequently, translational constraints are applied to all nodes of the mesh such that the mechanical assumptions that define L modes [3] are obeyed (Figs. 3(b) and (c)).

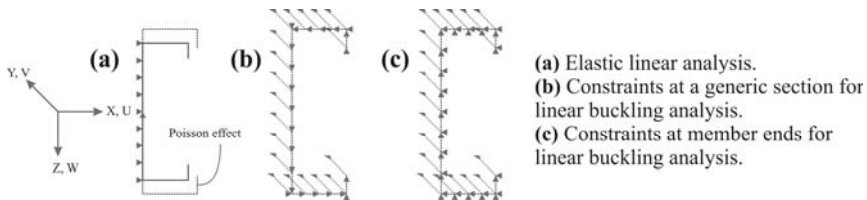


Figure 3: Direct constraining scheme for local deformation modes (S-S member).

The results obtained using the Fully scheme are close to FSM results, at least for buckling lengths of practical importance. For G mode, the difference is no more than 2% for lengths up to 5 meters, covering all the range where flexural-torsional mode is the controlling buckling state. For D mode, the difference is 2,73% for the 200 mm length, which is near the critical length. For L mode, the difference is 1,64% for the 70 mm length, near the critical one for this mode. The differences increase for lengths smaller than the critical for D mode and for long lengths for G mode. The 1 Sub scheme is an approximation of Fully, showing accuracy problems for lengths smaller than the critical for D mode. For L mode, the Direct scheme has provided the best results. However, such scheme can only be employed in an analysis considering only the first L mode. Therefore, the Direct scheme does not work in an analysis considering a specific individual deformation mode or a combination of modes.

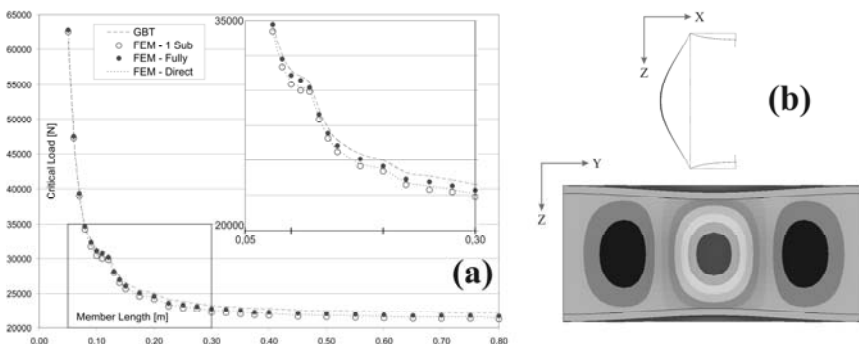


Figure 4: C-C member results. (a) Critical load of the first L mode. (b) Deformed shape of the 200 mm length member for combined mode calculation.

The critical loads of individual deformation modes have also been obtained for the C-C member, using the schemes 1 Sub and Fully (and also Direct for L mode). Similarly as for S-S member, the

*orthogonal axial modes* have been taken from CUFMSM routines, but the stiffness matrices have been modified to be compatible with the new boundary conditions.

Results for C-C member can not be compared with those provided by CUFMSM, since this software assumes that the longitudinal displacement distribution is sinusoidal, what is not compatible with C-C boundary conditions. Taking into account the more complex longitudinal displacement variation, the critical load results must be exhibited as a function of the member length. Fig. 4 shows the results for the first L mode. It is desirable to compare FEM results with those from FSM, since both methods employ the same element type. In despite of this, comparison with GBT results can give an idea of the validity of the method. The difference between Fully scheme and GBT is at most 4%, for the greater lengths.

Taking the first D mode and the first L mode from the *orthogonal axial modes* set (insets of Figs. 2(b) and 2(c)), the critical load of the combined mode has been calculated. A normalization scheme is needed in order to handle combined modes; two schemes have been considered herein: VN and WN. Tabs. 1 and 2 list some critical loads ( $P_{cr}$ ) of the combined mode for S-S and C-C members, comparing the results with those provided by cFSM and GBT. Only the results for 1 Sub constraining scheme are presented.

Table 1: Critical loads of combined mode calculation for the S-S member.

L [mm]	cFSM - WN			GBT	FEM - WN		
	$P_{cr}$ [N]	%D	%L	$P_{cr}$ [N]	$P_{cr}$ [N]	%D	%L
100	22870,3	19,5	80,5	22692,48	22571,4	23,6	76,4
150	26043,6	53,7	46,3	25373,02	24921,3	58,3	41,7
200	26932,8	73,3	26,7	26270,56	25876,4	75,6	24,4
300	34293,3	83,9	16,1	33921,07	33754,1	84,7	15,3
500	68869,7	86,9	13,1	68709,6	68886,4	87,3	12,7
800	158693,7	87,5	12,5	158590,2	159175,7	87,8	12,2

Table 2: Critical loads of combined mode calculation for the C-C member.

L [mm]	GBT			FEM - VN		
	$P_{cr}$ [N]	$r_D$	$r_L$	$P_{cr}$ [N]	%D	%L
100	29911,6	1	1	30247,6	10,24	89,76
150	25334,9	2	2	25529,9	7,78	92,22
200	23605,4	1	3	23773,7	36,79	63,21
300	21911,9	2	4	22057,0	36,31	63,69
500	21293,3	5	7	21434,7	23,40	76,60
800	21055,8	9	11	21212,6	20,12	79,88

For S-S member, the analyzed lengths represent the buckling length, which is the same for both individual deformation modes. The contributions of modes D and L (%D and %L) for S-S member have been compared with the values given by CUFMSM, for WN normalization scheme (which does not depend on the discretization). For C-C member, the analyzed lengths represent the member length, and the shape functions of the individual modes can have different numbers of half-waves. Again, C-C member results can only be compared with those of GBT. Based on the number of half-waves obtained for each individual mode in GBTUL ( $r_D$  e  $r_L$ ), the shape functions for these modes have been defined in the constrained finite element model. Recognizing that GBTUL does not employ the same normalization schemes of CUFMSM, the contributions comparison with FEM results has not been carried out.

The genetic algorithm method has only been employed in C-C member analysis, where the desired buckling mode is always the first. Results of Tab. 2 refer to an arbitrary algorithm run, and can be refined.

The critical load calculation of the combined mode with constraining scheme 1 Sub has yielded good results for the analyzed lengths. The greater difference has been 4,3% in comparison with cFSM, for the 150 mm length S-S member. The contributions of modes for S-S member calculated by FEM have shown a little difference in comparison with cFSM for the smaller lengths. This difference can be reduced if the

Fully constraining scheme, for instance, is used, since the 1 Sub scheme does not approximate well the critical loads of D mode for lengths smaller than the critical (Fig. 2(b)).

Different normalization schemes lead to different mode contributions results. VN scheme is dependent on the discretization and does not have physical meaning, what makes WN scheme preferable at first. However, the WN could not be used in C-C member analysis because, in general, each individual mode has a different associated geometric stiffness matrix. Therefore, the results of Tab. 2 refer to the VN scheme. It also should be observed that, in C-C member analysis, the consideration of a greater number of harmonic components of the shape functions may be important, as discussed in [6]. Fig. 4(b) illustrates the buckling mode of the 200 mm length C-C member for the combined mode calculation. It is clearly seen that there is a mix of a D mode taking place in one half-wave and a L mode with three half-waves.

## 5 CONCLUSION

This paper presents examples of critical load calculations of specific buckling modes of open cross-section thin-walled members by the use of the finite element method (FEM). In other words, it is possible to calculate the critical load of *individual deformation modes* belonging to groups of global, distortional, local or other modes. The calculation of any combination of modes can also be accomplished.

The numerical model is constrained such that its deformation fields are consistent with the desired mode, based on the concepts of constrained finite strip method (cFSM) [3]. The employed methodology is similar to that of Casafont *et al.* in [4]-[5], but the used individual modes have been the orthonormal modes suggested by Ádány and Schafer [3]. The procedure has been extended to other boundary conditions and to the evaluation of the contributions of individual modes in a general solution.

The individual and combined mode calculations using FEM have shown good results in comparison with those provided by cFSM and GBT, at least for buckling lengths and member lengths of practical importance. It should be pointed out that a study of more cross-sections is still needed.

The results presented herein mark the beginning of a longer research. The extension of cFSM concepts to FEM provides the ability of analyzing members with any boundary condition configuration and non-uniform members (e.g., members with holes).

## REFERENCES

- [1] Schafer, B.W. and Ádány, S., "Buckling analysis of cold-formed steel members using CUFSM: conventional and constrained finite strip methods", *18<sup>th</sup> International Specialty Conference on Cold-Formed Steel Structures*, Orlando, Florida, October 26-27, 2006.
- [2] Silvestre, N. and Camotim, D. "First-order generalised beam theory for arbitrary orthotropic materials". *Thin-Walled Structures*, **40**, 755-789, 2002.
- [3] Ádány, S. and Schafer, B.W. "A full modal decomposition of thin-walled, single-branched open cross-section members via the constrained finite strip method". *Journal of Constructional Steel Research*, **64**, 12-29, 2008.
- [4] Casafont, M., Marimon, F., Pastor, M.M. "Calculation of pure distortional elastic buckling loads of members subjected to compression via the finite element method". *Thin-Walled Structures*, **47**, 701-729, 2009.
- [5] Casafont, M., Pastor, M.M., Caamaño, E., Marimon, F., "Linear buckling analysis of compressed members combining the generalised beam theory and the finite element method", *Proceedings of the Twelfth International Conference on Civil, Structural and Environmental Engineering Computing*, Civil-Comp Press, Stirlingshire, Scotland, 2009.
- [6] Li, Z., *Buckling Analysis of the Finite Strip Method and Theoretical Extension of the Constrained Finite Strip Method for General Boundary Conditions*, Research Report, Johns Hopkins University, 2009.